Journal of Engineering Mathematics 21: 155–165 (1987)

Stability of viscous flow past a circular cylinder

A. ZEBIB
Department of Mechanical and Aerospace Engineering, Rutgers University, New Brunswick, NJ 08903, USA

Received 18 November 1986; accepted 8 January 1987

Abstract. A spectral method which employs trigonometric functions and Chebyshev polynomials is used to compute the steady, incompressible laminar flow past a circular cylinder. Linear stability methods are used to formulate a pair of decoupled generalized eigenvalue problems for the growth of symmetric and asymmetric (about the dividing streamline) perturbations. We show that, while the symmetric disturbances are stable, the asymmetric perturbations become unstable at a Reynolds number about 40 with a Strouhal number about 0.12. The critical conditions are found to depend on the size of the computational domain in a manner similar to that observed in the laboratory.

1. Introduction

It is well known that steady, laminar flow past a circular cylinder becomes unstable at a Reynolds number Re about 40. The early stages of the instability are observed as wake oscillations with a Strouhal number S less than about 0.12 (cf. Schlichting [8]). The recent experiments by Coutanceau and Bouard [2] indicate that the critical value Re_c for the onset of asymmetry (about the dividing streamline) is a strong function of the wall influences measured by the ratio of the cylinder diameter to that of the tank (λ). Experiments with λ equal 0.12, 0.07 and 0.024 showed instability at $\mathrm{Re}_c = 43$, 39.5 and 36, respectively. This increase of Re_c with λ reflects the stabilizing influence of the walls.

Computational studies have been largely concerned with the properties of the symmetric, laminar flow past a half cylinder. This, of course, excludes any asymmetric contribution and hence a steady state is always possible. Fornberg [3] gives a comprehensive review of the literature and addresses the problem of the treatment of the outflow boundary conditions. Finite-difference solutions of the time-dependent equations in the whole plane have been performed at $\mathrm{Re} \geqslant 100$ to study the development of a von Karman vortex street (cf. Jordan and Fromm [5]). Although solving the initial-value problem can be used to locate the onset of instabilities, it would be very expensive and does not seem to have been attempted. An alternative approach to computing the critical conditions is to predict the Hopf bifurcation point. Winters, Cliffe and Jackson [9] have just accomplished this task through the solution of an extended set of time-independent equations which they generate by a finite-element procedure. For their model boundary conditions, in particular at "infinity", they predict Re_c and S of 45.403 and 0.13626, respectively.

In this paper we determine the critical conditions by linear stability methods. We first compute the basic, steady, symmetric flow by a spectral method using trigonometric sine functions and Chebyshev polynomials as basis functions in the azimuthal and radial directions, respectively. Then we represent general two-dimensional disturbances in terms of both sine and cosine functions in the azimuthal direction. Linear stability analysis leads to

decoupled generalized matrix-eigenvalue problems for the growth of symmetric and asymmetric disturbances which we solve using standard methods.

We find the symmetric perturbations stable. These disturbances decay monotonically with a rate that is independent of Re in the range considered. The asymmetric disturbances become unstable at an Re value that depends on the size of the computational field, where these disturbances vanish, in a manner similar to that found experimentally by Coutanceau and Bouard [2]. The values of Re_c found range from 39 to 43 and those for S are between 0.11 and 0.13.

2. Mathematical formulation

The nondimensional Navier–Stokes equations are

$$\nabla \cdot \mathbf{v} = 0, \tag{1a}$$

$$\partial_t \mathbf{v} + (\mathbf{v} \cdot \nabla)\mathbf{v} = -\nabla p + \frac{2}{\mathrm{Re}} \nabla^2 \mathbf{v}. \tag{1b}$$

In (1), length, velocity $\mathbf{v}$, time t and pressure p have been assumed dimensionless with respect to the cylinder radius b, the free-stream velocity U, convective time b/U and dynamic pressure ϱU^2, respectively. The Reynolds number Re, based on the diameter $2b$, is $\mathrm{Re} = 2bU/\nu$, ϱ and ν are the fluid's density and kinematic viscosity, respectively. The motion is referred to the cylindrical coordinate system (Fig. 1), thus the boundary conditions are

$$\mathbf{v}(1, \theta, y, t) = \mathbf{0}, \tag{3a}$$

$$\mathbf{v}(r, \theta, y, t) = \mathbf{v}(r, \theta + 2\pi, y, t), \tag{3b}$$

$$\mathbf{v}(\infty, \theta, y, t) = (-\cos\theta, \sin\theta, 0). \tag{3c}$$

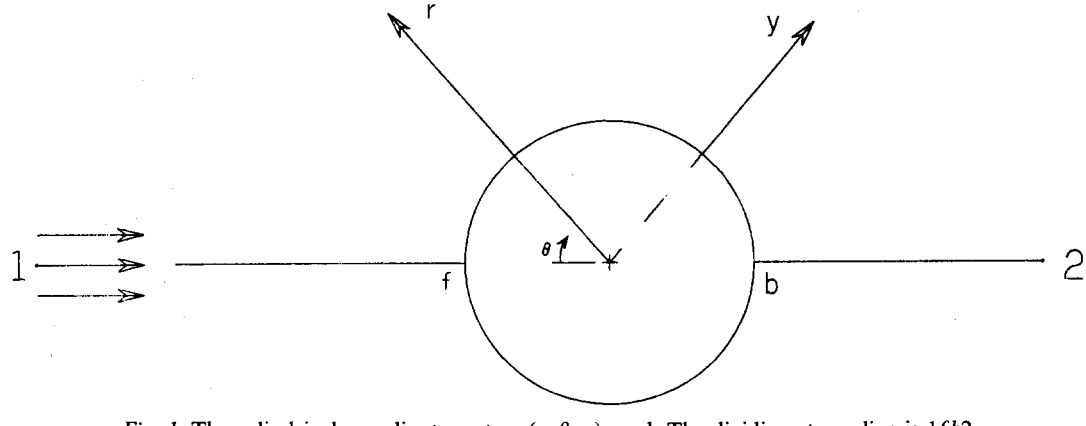

Fig. 1. The cylindrical coordinate system (r, θ, y) used. The dividing streamline is $1fb2$.

We represent the solenoidal velocity vector field in terms of two scalar functions $\Phi(\mathbf{r}, t)$ and $\Psi(\mathbf{r}, t)$ (Chandrasekhar [1]) so that the continuity equation (1a) is automatically satisfied:

$$\mathbf{v} = \nabla \times (\Psi \hat{e}_y) + \nabla \times (\nabla \times \Phi \hat{e}_y), \tag{4a}$$

$$= \left(\frac{1}{r}\partial_\theta \Psi, -\partial_r \Psi, 0\right) + \left(\partial^2_{yr}\Phi, \frac{1}{r}\partial^2_{y\theta}\Phi, -\nabla_1^2 \Phi\right), \tag{4b}$$

where ∇_1^2 is the two-dimensional, polar Laplacian and $\hat{e}_y$ is a unit vector in the y direction. The equations for Ψ and Φ are developed by first eliminating the pressure field by taking the curl of (1b) and using (1a),

$$\partial_t \boldsymbol{\omega} = \frac{2}{\mathrm{Re}} \nabla^2 \boldsymbol{\omega} + \nabla \times (\mathbf{v} \times \boldsymbol{\omega}), \tag{5}$$

where the vorticity $\boldsymbol{\omega} = \nabla \times \mathbf{v}$. The inner product of (5) and curl (5) with $\hat{e}_y$ leads to

$$\partial_t \nabla_1^2 \Psi = \frac{2}{\mathrm{Re}} \nabla^2 \nabla_1^2 \Psi - \hat{e}_y \cdot \nabla \times (\mathbf{v} \times \boldsymbol{\omega}), \tag{6a}$$

$$\partial_t \nabla^2 \nabla_1^2 \Phi = \frac{2}{\mathrm{Re}} \nabla^4 \nabla_1^2 \Phi + \hat{e}_y \cdot \nabla \times (\nabla \times (\mathbf{v} \times \boldsymbol{\omega})). \tag{6b}$$

In addition to the periodicity conditions (3b), the remaining boundary conditions (3a, c) are satisfied by requiring

$$\Psi = \partial_r \Psi = \Phi = \partial_r \Phi = \partial^2_{rr} \Phi = 0 \quad \text{at} \quad r = 1, \tag{7a}$$

$$\Psi \sim -r \sin\theta, \quad \Phi \sim 0 \quad \text{as} \quad r \to \infty. \tag{7b}$$

Equations (6–7), along with appropriate initial conditions, are to be solved for Ψ and Φ. Two-dimensional solutions are a special case with $\Phi \equiv 0$, in which case Ψ is the usual stream function of the motion.

3. Two-dimensional motions

Two-dimensional solutions are either steady and symmetric about the dividing streamline 1*fb*2 (Fig. 1) or unsteady. All of these solutions are obtained by solving (6a) for $\Psi(r, \theta, t)$ subject to the boundary conditions (7). With $\Phi \equiv 0$, the vorticity has a single nonzero component

$$\boldsymbol{\omega} = -\nabla_1^2 \Psi \hat{e}_y, \tag{8}$$

thus (6a) becomes

$$\partial_t \nabla_1^2 \Psi = \frac{2}{\mathrm{Re}} \nabla_1^4 \Psi - \frac{1}{r}\partial_\theta \Psi \partial_r \nabla_1^2 \Psi + \frac{1}{r}\partial_r \Psi \partial_\theta \nabla_1^2 \Psi. \tag{9}$$

A Fourier-series representation for Ψ which satisfies the periodicity conditions (3b) is

$$\Psi(r, \theta, t) = \sum_{n=0}^{\infty} f_n(r, t) \frac{1}{\sqrt{\pi}} \sin n\theta + g_n(r, t) \frac{1}{\sqrt{c_n \pi}} \cos n\theta, \tag{10}$$

where $f_n(r, t)$ and $g_n(r, t)$ are Fourier (spectral) coefficients to be determined and $c_0 = 2$, $c_n = 1$ for $n > 1$. We substitute the expansion (10) in (9) and take the Fourier inner products ($\int_0^{2\pi} \cdot \sin l\theta \, d\theta$ and $\int_0^{2\pi} \cdot \cos l\theta \, d\theta$) to obtain the initial/boundary-value problems for f_l and g_l:

$$\partial_t D_l f_l = \frac{2}{\mathrm{Re}} D_l^2 f_l + \frac{1}{r} \sum_{n,m=0}^{\infty} A_{mln} Q(f_m, f_n) - \frac{1}{\sqrt{c_n}} A_{nlm} Q(g_n, g_m), \tag{11a}$$

$$\partial_t D_l g_l = \frac{2}{\mathrm{Re}} D_l^2 g_l + \frac{1}{r} \sum_{n,m=0}^{\infty} B_{mln} Q(f_m, g_n) + C_{mln} Q(g_m, f_n), \tag{11b}$$

where the following definitions have been introduced for convenience

$$D_l = \frac{d^2}{dr^2} + \frac{1}{r}\frac{d}{dr} - \frac{l^2}{r^2}, \tag{11c}$$

$$Q(f_m, f_n) = D_m f_m \partial_r f_n - f_m \partial_r D_n f_n, \tag{11d}$$

$$A_{mln} = \frac{m}{\pi^{3/2}} \int_0^{2\pi} \cos m\theta \sin l\theta \sin n\theta \, d\theta, \tag{11e}$$

$$B_{mln} = \frac{m}{\pi^{3/2}\sqrt{c_l c_n}} \int_0^{2\pi} \cos m\theta \cos l\theta \cos n\theta \, d\theta, \tag{11f}$$

$$C_{mln} = \frac{-m}{\pi^{3/2}\sqrt{c_l}} \int_0^{2\pi} \sin m\theta \cos l\theta \sin n\theta \, d\theta. \tag{11g}$$

The boundary conditions (7) are satisfied by requiring

$$f_l = \partial_r f_l = g_l = \partial_r g_l = 0 \quad \text{at} \quad r = 1, \tag{12a}$$

$$f_l \sim -\sqrt{\pi} r \delta_{1l}, \quad g_l \sim 0 \quad \text{as} \quad r \to \infty, \tag{12b}$$

where δ_{lm} is the Kronecker delta. Because (11b) and the boundary conditions on g_l in (12) are homogeneous, an initial motion which is symmetric about the dividing streamline, i.e., with $g_l(r, 0) = 0$, $l \geqslant 0$, will continue to possess this symmetry, i.e., $g_l(r, t) = 0$, $t > 0$. As is well known, the experimentally observed motion at sufficiently low Re is symmetric and steady which implies that initially small values of $g_l(r, 0)$ will decrease in time so that the symmetric flow (given by the spectral components $f_l(r, t)$) is stable. While this may be asserted by solving the initial/boundary-value problem (11), (12) along with appropriate

initial conditions, we will demonstrate the stability characteristics of the basic steady flow by linear stability methods.

3.1. Steady two-dimensional flow

Here the flow is symmetric about the dividing streamline and $g_l(r, t) = 0$, $l \geqslant 0$. Thus the motion is given by

$$\Psi(r, \theta) = \sum_{n=1}^{N_\theta} f_n(r) \frac{1}{\sqrt{\pi}} \sin n\theta, \tag{13}$$

where

$$0 = \frac{2}{\mathrm{Re}} D_l^2 f_l + \sum_{n,m=1}^{N_\theta} \frac{1}{r} A_{mln} Q(f_m, f_n), \tag{14a}$$

$$f_l(1) = f_l'(1) = 0 \quad \text{and} \quad f_l(r \to \infty) \sim -\sqrt{\pi} r \delta_{1l} \tag{14b, c}$$

along with definitions (11c–e), and primes denote differentiation with respect to argument. In (13) the infinite sum has been truncated to N_θ terms. Solution of the N_θ coupled nonlinear system (14a, b) has been described in detail (Zebib [10]). Here we only give a brief account of the solution procedure. The radially infinite computational domain is truncated to the finite region

$$r_\infty = \mathrm{e}^a, \quad \text{for some } a. \tag{15}$$

Because the differential equations for $f_l(r)$ are of fourth order we need two conditions for each f_l at r_∞. We cannot impose the asymptotic free-stream condition $f_l(r_\infty) = -\sqrt{\pi} r_\infty \delta_{1l}$ as this implies no wake at r_∞. An accurate boundary condition which is easy to implement (Fornberg [3]) are the soft conditions

$$f_l' = -\sqrt{\pi}\delta_{1l} \quad \text{and} \quad f_l''' = 0, \quad \text{at} \quad r = r_\infty. \tag{16}$$

We can replace $f_l'''(r_\infty) = 0$ by $f_l''(r_\infty) = 0$ with no appreciable difference in the computed results.

Solutions of (14a, b) and (16) are constructed by a spectral method using Chebyshev polynomials $T_i(z)$, $-1 \leqslant z \leqslant 1$. We first introduce the transformation

$$r = \exp\left[\frac{a}{2}(z + 1)\right], \tag{17}$$

so that $1 \leqslant r \leqslant \mathrm{e}^a$ (see (15)) implies $-1 \leqslant z \leqslant 1$. Next we develop the Chebyshev expansions for $f_l(z)$ and its derivatives $f_l^{(\beta)}(z)$, $\beta = 0, 1, 2, 3, 4$,

$$f_l^{(\beta)}(z) = \sum_{j=0}^{N_r+4-\beta} \sum_{i=0}^{N_r} G_{ji}^{(\beta)} a_{li} T_j(z) + \delta_{1l} \sum_{j=0}^{3} b_j^{(\beta)} T_j(z). \tag{18}$$

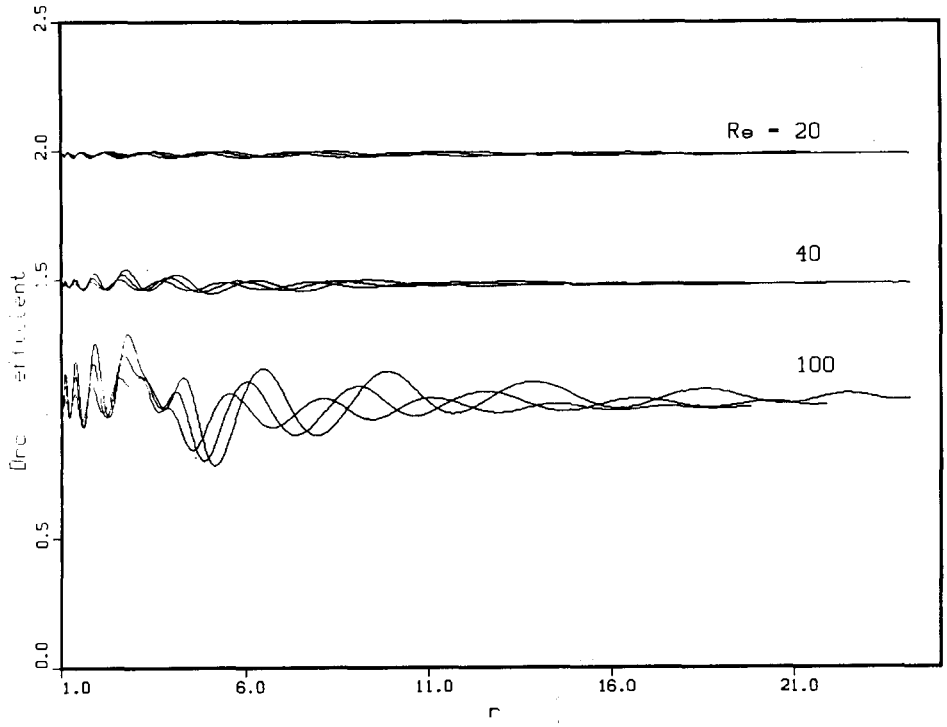

Fig. 2. Variation of the drag coefficient with radial position of control volume. Results for Re = 20, 40 and 100, a = 3, 3.1 and 3.2 are shown for N_r = 23 and N_θ = 44. Accuracy to within 4% at Re $\leqslant$ 40 is indicated.

Here N_r is the truncation number in the radial (z) direction and a_{li} are the spectral coefficients to be computed. The matrices $G_{ji}^{(\beta)}$, $\beta = 0, \ldots, 4$ are developed from the recurrence relations of $T_j(z)$ in such a way that the homogeneous version of the boundary conditions (14b) and (16) is satisfied, i.e.,

$$\sum_{j=0}^{N_r+4}\sum_{i=0}^{N_r} G_{ji}^{(0)} a_{li}(-1)^j = \sum_{j=0}^{N_r+3}\sum_{i=0}^{N_r} G_{ji}^{(1)} a_{li}(\pm 1)^j = \sum_{j=0}^{N_r+1}\sum_{i=0}^{N_r} G_{ji}^{(3)} a_{li} = 0, \tag{19}$$

while the cubic polynomials with coefficients $b_j^{(\beta)}$, $\beta = 0, \ldots, 4$ satisfy the nonhomogeneous boundary conditions (14c) and (16).

The representations (18) are introduced into the boundary-value problem (14a) and the Chebyshev inner products with $T_i(z)$, $i = 0, 1, \ldots, N_r$ performed (i.e., we equate coefficients of $T_i(z)$ in the resulting equations). Thus we have to solve a nonlinear algebraic system of equations of the form

$$\sum_{m=1}^{N_\theta}\sum_{j=0}^{N_r} L_{limj} a_{mj} + B_{li} = \sum_{m,n=1}^{N_\theta}\sum_{j,k=0}^{N_r} N_{limjnk} a_{mj} a_{nk}, \quad l = 1, 2, \ldots, N_\theta, \quad i = 0, 1, \ldots, N_r, \tag{20}$$

to determine the spectral coefficients a_{li}. This we do by Newton's iteration.

The accuracy of the solutions is a strong function of r_∞ and the truncation parameters N_r and N_θ. As Re increases more Fourier functions are needed to represent the wake and as r_∞ increases more Chebyshev polynomials are required to resolve the radial direction. Our numerical experiments showed that sufficiently accurate solutions for Re about 40 or less may be obtained with $N_\theta \simeq 40$, $N_r \simeq 20$ and $r_\infty \simeq 20$. As the properties of the symmetric steady states are well documented in the literature, we only show the variation of the drag coefficient c_d with r as computed at different values of Re, r_∞, N_r and N_θ. We calculate c_d by integrating the momentum equation (1b) over a cylindrical control volume located at radius r which yields

$$c_d = \frac{\sqrt{\pi}}{2r}\left\{\sum_{n,m=1}^{N_\theta} A_{nlm}(2f_n'f_m' + 4m^2 f_n f_m + 2f_n f_m' - 2f_n f_m'') + \frac{4}{\mathrm{Re}}(f_1''' - 3f_1'' - f_1' + 3f_1)\right\}. \tag{21}$$

Figure 2 shows the influence of Re and r_∞ on the variation of c_d with r. We plot results with $(N_r, N_\theta) = (22, 44)$ at $a = 3$, 3.1 and 3.2 (i.e., $r_\infty \simeq 20.1$, 22.2 and 24.5, respectively) corresponding to Re of 20, 40 and 100. While there is virtually no variation of c_d with r at $\mathrm{Re} = 20$ ($c_d \simeq 1.99$), there is a maximum variation of about 4% at $\mathrm{Re} = 40$ ($c_d \simeq 1.49$). We include the result for $\mathrm{Re} = 100$ to demonstrate the deterioration of accuracy with increasing Re, especially close to the cylinder. From Fig. 1, however, we claim accurate solutions at Re less than or equal to 40.

4. Two-dimensional instability of the steady two-dimensional solutions

Instability of the steady, two-dimensional solutions is determined from linear theory. The basic motion satisfies (see (13, 14))

$$\bar{\Psi}(r, \theta) = \sum_{n=1}^{N_\theta} \bar{f}_n(r) \frac{1}{\sqrt{\pi}} \sin n\theta, \tag{22}$$

$$0 = \frac{2}{\mathrm{Re}} D_l^2 \bar{f}_l + \sum_{n,m=1}^{N_\theta} \frac{1}{r} A_{mln} Q(\bar{f}_m, \bar{f}_n). \tag{23}$$

We consider a general infinitesimal two-dimensional disturbance given by a stream function $\Psi'(r, \theta, t)$ of the form (10),

$$\Psi'(r, \theta, t) = \sum_{n=0}^{N_\theta'} f_n'(r, t) \frac{1}{\sqrt{\pi}} \sin n\theta + g_n'(r, t) \frac{1}{\sqrt{c_n \pi}} \cos n\theta, \tag{24}$$

where the number of azimuthal modes N_θ' required for accurate computation of Ψ' need not be equal to N_θ and is found by carrying out numerical experiments. We now substitute $\bar{\Psi} + \Psi'$ for Ψ in (9), and after linearization we derive the equations for the Fourier components, $0 \leqslant l \leqslant N_\theta'$,

$$\partial_t D_l f_l' = \frac{2}{\mathrm{Re}} D_l^2 f_l' + \frac{1}{r} \sum_{n=1}^{N_\theta'} \sum_{m=1}^{N_\theta} A_{mln} Q(\bar{f}_m, f_n') + A_{nlm} Q(f_n', \bar{f}_m), \tag{25}$$

$$\partial_t D_l g_l' = \frac{2}{\mathrm{Re}} D_l^2 g_l' + \frac{1}{r} \sum_{n=0}^{N_0'} \sum_{m=1}^{N_\theta} B_{mln} Q(\bar{f}_m, g_n') + C_{nlm} Q(g_n', \bar{f}_m). \tag{26}$$

From (25) and (26) it is evident that growth or decay of symmetric and asymmetric perturbations (i.e., f_l' and g_l', respectively) are determined from decoupled equations and can be evaluated separately.

4.1. Symmetric disturbances

The boundary conditions on $f_l'(r, t)$ follow from (12a) and (16); thus we require

$$f_l' = \partial_r f_l' = 0 \quad \text{at} \quad r = 1, \tag{27a}$$

$$\partial_r f_l' = \partial_r^3 f_l' = 0 \quad \text{at} \quad r = \mathrm{e}^a, \tag{27b}$$

so that f_l' has the representation (see (18), (19))

$$\partial_r^{(\beta)} f_l'(r, t) = \sum_{j=0}^{N_r'+4-\beta} \sum_{i=0}^{N_r'} G_{ji}^{(\beta)} a_{li}'(t)\, T_j(z), \tag{28}$$

where the truncation N_r' need not equal to N_r.

The initial-value problem for $a_{li}'(t)$ is derived by substituting (28) in (25) and performing the Chebyshev inner product with basis functions $\phi_i(z)$, $0 \leqslant i \leqslant N_r'$, which yields

$$\sum_{m=1}^{N_0'} \sum_{j=0}^{N_r'} B_{limj} \partial_t a_{mj}' = \sum_{m=1}^{N_0'} \sum_{j=0}^{N_r'} A_{limj} a_{mj}'. \tag{29}$$

The choice of the basis function $\phi_i(z)$ is important. If we use the obvious basis, $T_i(z)$, the resulting eigenvalue problem is found to have a number of spurious eigenmodes equal to N_0'. This situation is found in other stability problems described by the Orr-Sommerfeld equations (Gottlieb and Orszag [4], Zebib [10]). A remedy for these spurious roots has been described in Zebib [11]. We simply chose for $\phi_i(z)$ a basis which satisfies all of the homogeneous boundary conditions satisfied by the perturbations. Thus we take

$$\phi_i(a) = \sum_{j=0}^{N_r'+4} G_{ji}^{(0)} T_j(z), \tag{30}$$

which satisfies (27). The solution of (29) is found in the usual way by letting

$$a_{mj}' = \mathrm{e}^{\pi(\sigma + iS)t} c_{mj} \tag{31}$$

in (29) and solving the resulting generalized eigenvalue problem by standard library subroutines. It should be noted that the factor π in the exponent of (31) is used so that S is the Strouhal number based on the diameter (recall that the length scale in (1) is the radius).

We found that the symmetric disturbances are stable as expected. The eigenmode with slowest decay is monotonic ($S = 0$) with $\sigma \approx -0.01$ for Re less than 60. This results from

computations with N_r, N_0 and N_r', N_0' up to (22, 44) and (14, 40), respectively, at the r_∞ value of Fig. 1.

4.2. Asymmetric disturbances

Here we insist that asymmetric perturbations decay to zero at r_∞. This is so to ensure symmetric inflow at r_∞. Thus the proper boundary conditions on $g_l'(r, t)$, according to (12) are

$$g_l' = \partial_r g_l' = 0 \quad \text{at} \quad r = 1 \text{ and } r_\infty. \tag{32}$$

We now construct a representation for $g_l'(r, t)$ in terms of $T_j(z)$ in a manner similar to that leading to (28),

$$\partial_r^{(\beta)} g_l'(r, t) = \sum_{j=0}^{N_r'+4-\beta} \sum_{i=0}^{N_r'} F_{ji}^{(\beta)} b_{li}'(t)\, T_j(z), \tag{33}$$

with $F_{ji}^{(\beta)}$, $\beta = 0, \ldots, 3$, developed so that the boundary conditions in (32) are identically satisfied. The algebraic eigenvalue problem is derived in a manner similar to that leading to (29). Here, however, the basis functions $\phi_i(z)$ (see (30)) are

$$\phi_i(z) = \sum_{j=0}^{N_r'+4} F_{ji}^{(0)} T_j(z), \tag{34}$$

so that $\phi_i(z)$ satisfy all of the homogeneous conditions in (32). The generalized eigenvalue problem is then derived by letting

$$b_{li}'(t) = e^{\pi(\sigma + iS)t}\, d_{li}, \tag{35}$$

for $0 \leqslant l \leqslant N_0'$ and $0 \leqslant i \leqslant N_r'$.

The results of the computations are shown in Fig. 3, where we plot σ and S for the fastest growing mode as a function of Re corresponding to the r_∞ values of Fig. 1. The computations are with (N_r, N_0) and (N_r', N_0') at (22, 44) and (14, 30), respectively. The accuracy of these results have been confirmed by performing computations at lower truncations. Figure 3 shows the variation of σ and S with Re at fixed r_∞. At the lowest values of Re, about 10, the least stable mode has an S about 0.06. With increasing Re the eigenmode with S about 0.1 becomes the least stable, i.e., its σ increases and dominates the σ associated with other eigenmodes). This mode switching occurs at Re about 25, depending on the value of r_∞. The second mode switching, with $S = 0.13$, takes place where the flow becomes unstable at Re_c in the range 39–43. The flow is unstable for $\mathrm{Re} > 45$.

It is also evident from Fig. 3 that the smaller the value of r_∞ where the asymmetric disturbances vanish (in fact satisfy the no-slip conditions (32)) the more stable is the flow and the higher is the value of Re_c. This is consistent with the experimental results of Coutanceau and Bouard [2]. In addition, the increase of S with Re, which we find due to exchange of eigenmodes, is in qualitative agreement with observations (cf. Schlichting [8]).

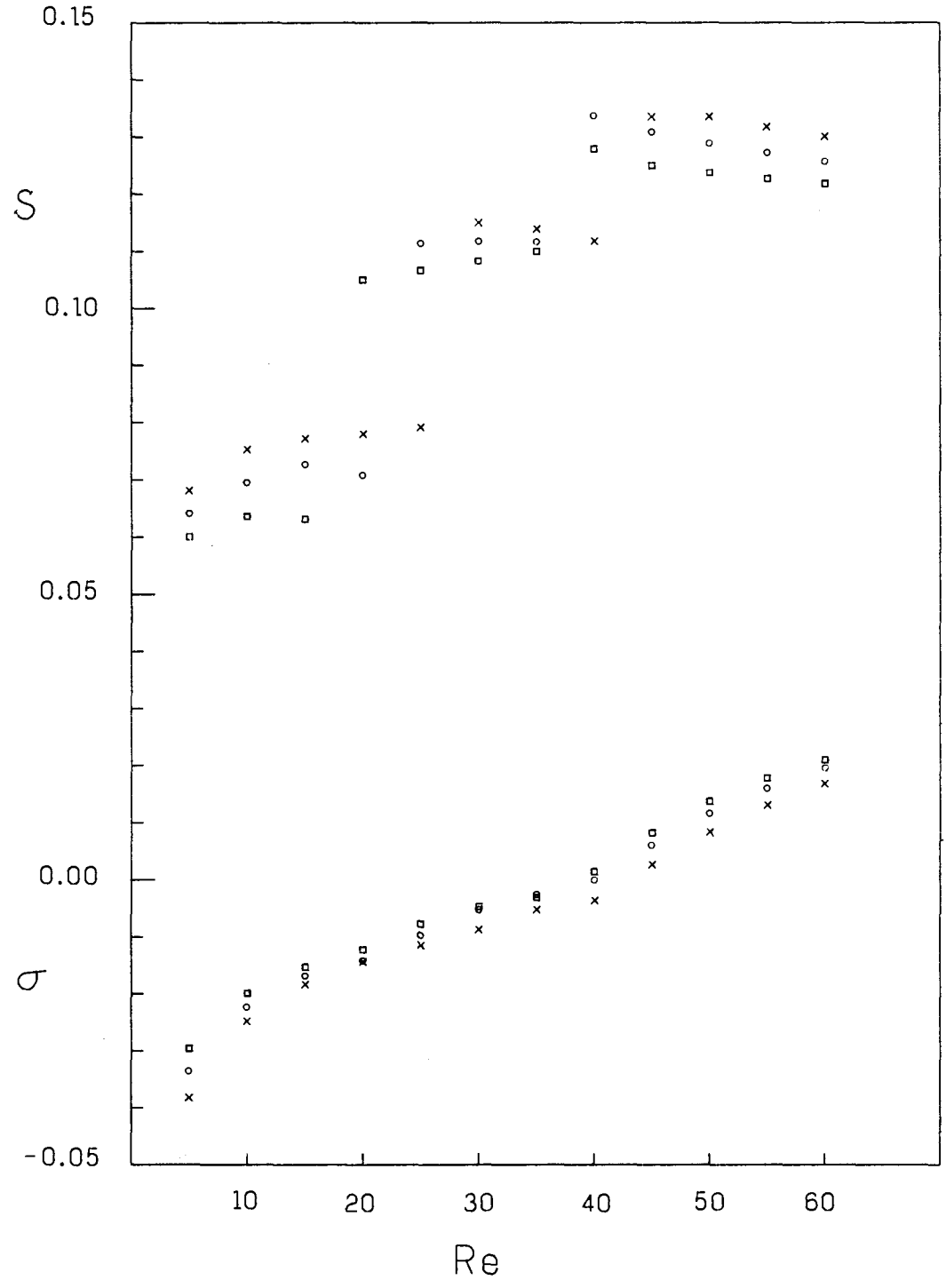

Fig. 3. The bifurcation diagram for asymmetric perturbations. σ is the growth rate of the most dangerous mode and S is its associated Strouhal number. ×, $a = 3$; ○, $a = 3.1$ and □, $a = 3.2$. Re_c, S are in the ranges 39–43 and 0.11–0.13, respectively.

5. Concluding remarks

We have carried out a linear stability analysis of the steady flow past a circular cylinder. The basic flow is two-dimensional and the disturbances are also two-dimensional but include asymmetric contributions. The theoretically obtained results are shown to be in good agreement with experiments.

There is a need for successful theoretical prediction of the three-dimensional instabilities which form near the frontal stagnation point of the cylinder. Existing theoretical studies have so far been concerned with the Hiemenz solution as the basic flow (cf. Lyell and Huerre [6]). Our mathematical formulation in equations (1) to (6) is general and allows for stability analysis of three-dimensional perturbations with Φ nonzero but small. However, we need to be able to compute accurate steady, symmetric flow at Re $\sim$ 1000. We have shown that a spectral representation with about 1000 spectral coefficients is needed to accurately describe the flow at Re $\approx$ 40. This solution is obtained in about 1.5 minutes on a CYBER 205. However, because the Jacobian of (20) is full, we did need one million 64 bit words of memory. Thus, in order that we may proceed further, we must develop a method following the ideas of Orszag [7] to construct a sparse approximate Jacobian to (20). This is currently in progress.

Acknowledgements

Funds for the support of this study have been allocated by the NASA-Ames Research Center, Moffet Field, California, under interchange No. NCA2-61. Computer time on the CYBER 205 has been provided by an NSF Grant through the John von Neumann Supercomputer Center, Princeton, NJ.

References

1. S. Chandrasekhar, *Hydrodynamic and Hydromagnetic Stability*, Clarendon Press, Oxford (1961), p. 24.
2. M. Coutanceau and R. Bouard, Experimental determination of the viscous flow in the wake of a circular cylinder in uniform translation, *J. Fluid Mech.* 79 (1977) 231–256.
3. B. Fornberg, A numerical study of steady viscous flow past a circular cylinder, *J. Fluid Mech.* 98 (1980) 819–856.
4. D. Gottlieb and S.A. Orszag, *Numerical Analysis of Spectral Methods*, NSF-CMBS Monograph No. 26, Soc. Ind. and App. Math, Philadelphia, PA (1977), pp. 144, 145.
5. S.K. Jordan and J.E. Fromm, Oscillatory drag, lift, and torque on a circular cylinder in a uniform flow, *Phys. Fluids* 15 (1972) 371–376.
6. M.J. Lyell and P. Huerre, Linear and nonlinear stability of plane stagnation flow, *J. Fluid Mech.* 161 (1985) 295–312.
7. S.A. Orszag, Spectral methods for problems in complex geometries, *J. Comp. Phys.* 37 (1980) 70–92.
8. H. Schlichting, *Boundary Layer Theory*, McGraw Hill (1979), pp. 31, 32.
9. K.H. Winters, K.A. Cliffe and C.P. Jackson, The prediction of instabilities using bifurcation theory, to appear in *Numerical Methods in Transient and Coupled Systems*, John Wiley (1986).
10. A. Zebib, A Chebyshev method for the solution of boundary value problems, *J. Comp. Phys.* 53 (1984) 443–455.
11. A. Zebib, 1986, Removal of spurious modes encountered in solving stability problems by spectral methods, to appear in *J. Comp. Phys.*